JOURNAL OF MATERIALS SCIENCE 40 (2005) 5199–5206

Preparation of acetylcellulose/silica composites by sol-gel method and their mechanical properties

K. TANAKA, H. KOZUKA
Department of Materials Science and Engineering, Kansai University, 3-3-35 Yamate-cho, Suita, 564-8680, Japan
E-mail: kozuka@ipcku.kansai-u.ac.jp

Acetylcellulose (AC)/silica composites were prepared by sol-gel method in an attempt to realize materials with Young's moduli and bending strengths similar to those of cortical bones. $Si(OCH_3)_4$ (TMOS)-AC-H_2O-HNO_3-tetrahydrofuran-$CH_3OC_2H_4OH$ solutions were allowed to be gelled, where AC/TMOS mole ratios were defined for AC monomers, and the gels were dried at 30–70°C to obtain composites. The composites prepared from solutions of mole ratios of AC/TMOS = 0.5 and 1.0 were composed of micrometer-sized particles rich in silica surrounded by the matrix rich in AC. The composites from solutions of AC/TMOS = 2.0, on the other hand, the interface between the particles and the matrix was much less distinct. All the composite samples showed good machinability, which could be cut into 5 mm × 2 mm × 4.4 mm rectangular specimens by an electric saw without cracking or fracture. The specimens were subjected to three-point bending test, where the degree of plastic deformation and the fracture strain increased, and Young's modulus and bending strength decreased with increasing AC/TMOS ratio in the starting solutions. When the gels were dried at higher temperatures, Young's modulus and strength increased. Young's modulus and bending strength could be varied in the range of 1.8–3.9 GPa and 48–100 MPa, respectively, by varying the AC/TMOS ratio in solutions and the drying temperature.

1. Introduction

Artificial bones need to have bioactivity, biocompatibility and mechanical properties similar to those of natural bones. Metallic or inorganic artificial bones proposed so far include Ti-Al-V alloys, Cr-Co-Mo alloys, stainless steel (316L), glass-ceramics (AW and Bioverit®, sintered hydroxyapatite, alumina, zirconia and silicon nitride. These materials have Young's moduli of 70–420 GPa [1, 2], which are higher than those of cortical bones (7–30 GPa) and cancellous bones (0.05–0.5 GPa) [2]. In an attempt to realize artificial bones with Young's moduli similar to those of natural bones, recently a variety of organic-inorganic composite materials have been prepared, bearing in mind that the natural bones are composed of collagen fibers and carbonate-containing hydroxyapatite [3]. Kobayashi *et al.* [4] prepared (AW, hydroxyapatite (HAp), tricalcium phosphate)/bisphenol-a-glycidylmethacrylate triethyleneglycol dimethacrylate composites, 4–12 GPa in Young's modulus and 50–130 MPa in bending strength. Kasuga *et al*. [5] prepared HAp/poly-L-lactic acid composites having Young's moduli of 4–11 GPa and bending strengths of 40–60 MPa. These composites can be said to have similar mechanical properties to those of cortical bones, 7–30 GPa and 50–150 MPa in Young's modulus and bending strength, respectively. As far as the materials with mechanical properties comparable to cancellous bones, Kamitakahara *et al*. [6] prepared CaO-SiO_2/polydimethylsiloxane (PDMS) composites, and Chen *et al*. [7–9] proposed CaO-SiO_2-TiO_2/PDMS composites. Besides organic-inorganic composite materials to be used as artificial bones include SiO_2/polymethylmethacrylate (PMMA) [10, 11], HAp/PMMA [12], Bioglass®/high-density polyethylene (HDPE) [13, 14], AW/HDPE [15], HAp/polyethylene [16], HAp/poly-L-lactide (PLLA) [17], calcium phosphate/copolymer PLLA [18], $CaCO_3$/polylactic acid [19], and $50CaO{\cdot}50SiO_2$/PMMA [20] composites. They had Young's moduli, bending strengths and tensile strengths ranging over 0.65–71 GPa and 64–280 MPa, 10–94 MPa, respectively. Although not attempted to be used as artificial bones, a number of organic-inorganic composites have been prepared and subjected to mechanical property measurements. For instance, Mackenzie's group prepared organically modified silicates (ormosils) from PDMS and $Si(OC_2H_5)_4$, demonstrating that the flexibility increases with increasing PDMS contents [21–23]. Also reported are SiO_2/hydroxypropyl cellulose [24], SiO_2/polyvinylacetate [25], SiO_2/polyimide [26, 27], SiO_2/PDMS [28, 29], SiO_2/polyvinyl alcohol [30],

0022–2461
DOI: 10.1007/s10853-005-4413-2

SiO_2/polytetramethylene oxide [31], and (Ta_2O_5, ZrO_2)/PDMS [32] composites, which had Young's moduli and bending strengths ranging over 6×10^5–3.5 GPa and 0.06–143 MPa, respectively.

Composites containing organic polymers that have bioresorption property are expected to be integrated with natural bones in the body, where the bone tissue penetrates into the pores left behind by the polymers dissolved [33]. Polylactic acid and cellulose are known to have bioresorption property, and the examples are found in the literature on HAp/polylactic acid [17], and calcium phosphate/polylactic acid [18] composites. In the present work, acetylcellulose (AC), an organic polymer with bioresorption property [34], and SiO_2, a bioactive and biocompatible material [35], were combined to fabricate organic-inorganic composites by sol-gel method. Formation, microstructure, and mechanical properties of bulk composites were studied where the effects of the AC content and drying temperature on mechanical properties were focused on.

2. Experimental

2.1. Preparation

Tetramethylorthosilicate (TMOS) $Si(OCH_3)_4$ (Tokyo Kasei Kogyo, Tokyo, Japan), tetrahydrofuran (THF) (Wako Pure Chemical Industries, Osaka, Japan), ion-exchanged water, 1 M nitric acid (Wako Pure Chemical Industries), acetylcellulose (AC) (acetylation 53–56%, average molecular weight 288, Wako Pure Chemical Industries), and 2-methoxyethanol $CH_3OC_2H_4OH$ (Wako Pure Chemical Industries) were used as the starting materials. Starting solutions of mole ratios listed in Table I were prepared where the mole ratio for AC was defined for the monomer. Hereafter the solutions of AC/TMOS mole ratios of 0.5, 1.0 and 2.0 are called AC0.5, AC1 and AC2, respectively. H_2O - nitric acid - THF solution was added to TMOS - THF solution under magnetic stirring, and then ground AC powders and $CH_3OC_2H_4OH$ were added in this sequence. Transparent 500 mL solution thus obtained was poured in a polyethylene container 10 cm × 15 cm × 5.5 cm in dimension, the inner of which was coated beforehand with grease (HP-500, Dow Corning Asia, Tokyo, Japan) in order to allow the gel/container separation with ease. A lid with 15 holes 3 mm in diameter was placed on the container, and the solution was kept at 30°C for 10 days where the solution was allowed to be gelled. The gel plates obtained were placed on a stainless wire netting, and then were further dried either at 30, 50 or 70°C for 35 days. Hereafter the drying on the stainless wire netting is called post-drying.

The dried gels obtained were cut with an electric saw and polished with #200 emery paper into rectangular specimens ca. 5 mm × 2 mm × 4.4 mm in dimension.

TABLE I Compositions of the starting solutions

	Mole ratio					
Solution	TMOS	AC	H_2O	HNO_3	THF	$CH_3OC_2H_4OH$
AC0.5	1	0.5	10	0.01	26.4	2.53
AC1	1	1.0	10	0.01	26.4	2.53
AC2	1	2.0	10	0.01	32.0	2.53

2.2. Measurement and observation

The bulk density was calculated on the rectangular specimens from the weight and the dimensions. The rectangular specimens were subjected to three-point bending test performed in the ambient atmosphere using a universal testing machine (Model 4302, Instron Japan, Tokyo, Japan). The measurements were conducted with a three-point loading over a 40 mm span at a crosshead speed of 1.00 mm min^{-1}, where six to eleven specimens were served for the measurements. The displacement and load data were converted into strain and stress, respectively, using the following equations [36];

$$\sigma = \frac{3PL}{2bh^2} \times 9.8 \quad (1)$$

$$\varepsilon = \frac{6hY}{L^2} \quad (2)$$

where σ (MPa) in the stress, P (kgw) the load, L (mm) the span, Y (mm) the displacement, b (mm) the specimen width, h (mm) the specimen thickness. Young's modulus and bending strength were obtained from the slope and the maximum stress in the stress-strain curves.

The fracture surface of the specimens was observed with a scanning electron microscope (SEM) (Model JSM-T20S, JEOL, Tokyo, Japan). Element analysis was also conducted using an energy dispersive X-ray spectrometer (EDX) (Model JED-2200, JEOL) attached to the SEM.

3. Results

3.1. Appearance and machinability of the dried gel plates

Slightly yellow, opaque, crack-free dried gel plates ca. 12 cm × 6.5 cm × 0.8 cm in dimension were formed irrespective of the AC/TMOS ratio by keeping the sols at 30°C for 10 days in the polypropylene container. Unless $CH_3OC_2H_4OH$ is added to the starting solution, the gel plates are warped during drying. Addition of $CH_3OC_2H_4OH$ in the starting solutions is indispensable for avoiding the warping on drying.

Fig. 1 shows the photograph of a composite specimen subjected to post-drying at 70°C followed by cutting

Figure 1 Photograph of the composite specimen prepared from solution AC1 and post-dried at 70°C.

and polishing. All the composite specimens exhibited good machinability irrespective of AC/TMOS ratio and post-drying temperature, i.e., they could be cut and polished without cracking.

3.2. Composites subjected to post-drying at different temperatures

Fig. 2 shows the dependence of bulk density on post-drying temperature for the composite samples prepared from solution AC1. The bulk density of the composites increased by about 8% from 1.22 ± 0.05 to 1.31 ± 0.04 g cm^{-3} with increasing post-drying temperature from 30 to 70°C.

The stress-strain curves and fracture strain data are shown in Fig. 3 and Table II, respectively, for these composite samples prepared from solution AC1 and post-dried at different temperatures. The composites exhibited residual strain, i.e. permanent deformation after removal of stress. As seen in Fig. 3, the composite samples exhibited elastic deformation followed by plastic deformation, where plastic deformation was

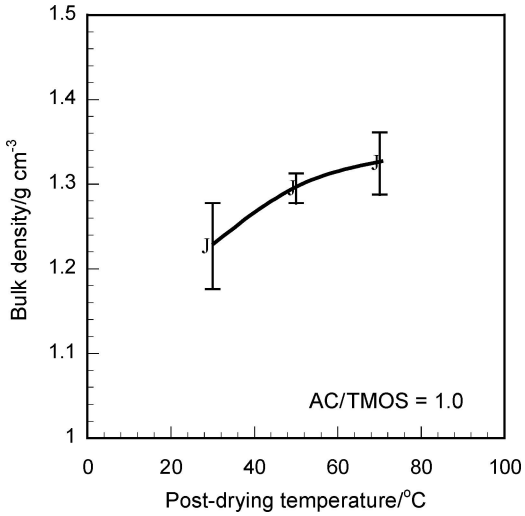

Figure 2 Bulk density plotted against post-drying temperature for the composites prepared from solution AC1.

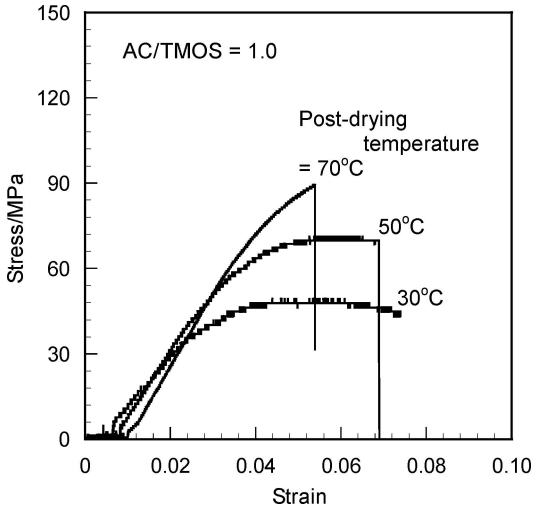

Figure 3 Stress–strain curves of the composites post-dried at different temperatures. The composites were prepared from solution AC1.

TABLE II Fracture strain of the composite samples prepared from solutions of various AC/TMOS mole ratio and by post-drying at various temperatures

AC/TMOS mole ratio	Post-drying temperate (°C)	Fracture strain (%)
1.0	30	>6.8
1.0	50	6.6 ± 0.7
1.0	70	5.7 ± 1.3
0.5	70	3.9 ± 0.3
1.0	70	5.7 ± 1.3
2.0	70	>8.0

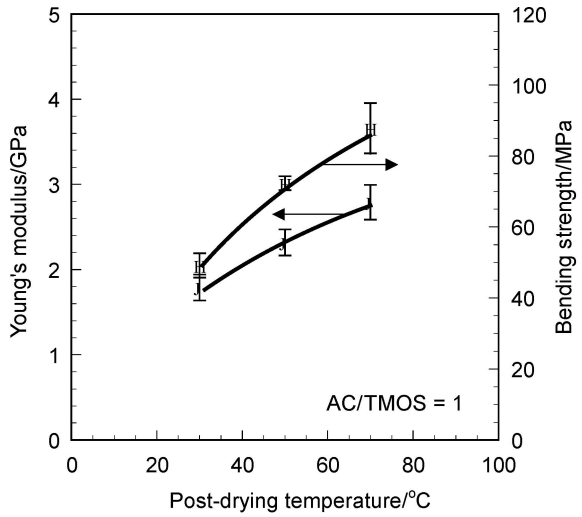

Figure 4 Young's modulus and bending strength plotted against post-drying temperature for the composites prepared from solution AC1.

found in smaller strain ranges for the composites post-dried at higher temperatures. The fracture strain was larger than 6.8% for the composite samples post-dried at 30°C (Table II) where the strain was over the measurement limitation of the tester. As seen in Table II, the fracture strain decreased from over 6.8% to 5.7 ± 1.3% when the post-drying temperature increased from 30 to 70°C, showing smaller fracture strain for the composites post-dried at higher temperatures.

Young's moduli and bending strengths obtained from the strain-stress curves are shown in Fig. 4 as a function of post-drying temperature. Young's modulus increased by about 56%, from 1.8 ± 0.2 to 2.8 ± 0.2 GPa, when the post-drying temperature increased from 30 to 70°C. The bending strength increased by about 78% from 49 ± 3 to 88 ± 7 MPa with increasing post-drying temperature from 30 to 70°C.

3.3. Composites prepared from solutions of different AC/TMOS ratios

Fig. 5 shows the bulk density of the composites plotted against AC/TMOS ratio in the starting solutions, where the gels were post-dried at 70°C. The bulk density decreased by about 5%, from 1.37 ± 0.05 to 1.29 ± 0.04 g cm^{-3}, with increasing AC/TMOS mole ratio from 0.5 to 2.0 although it was nearly the same between the samples from solutions of AC/TMOS = 1.0 and 2.0.

The strain-stress curves and fracture strain data of these composite samples are shown in Fig. 6 and

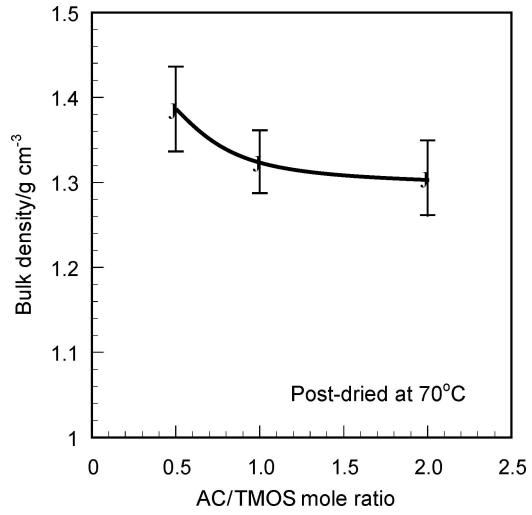

Figure 5 Bulk density of the composites plotted against AC/TMOS mole ratio. The composites were post-dried at 70°C.

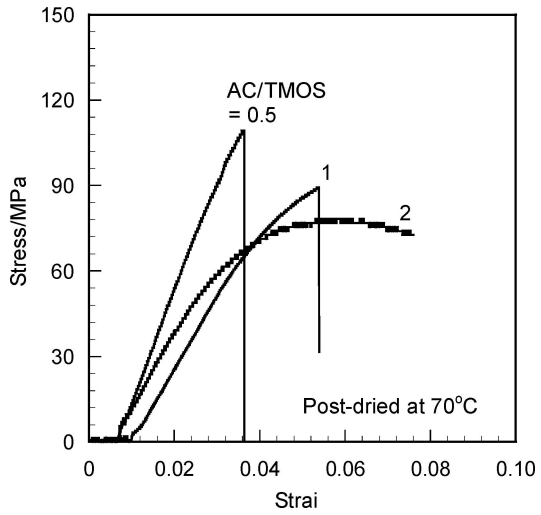

Figure 6 Stress–strain curves of the composite specimens prepared from solutions of different AC/TMOS mole ratios. The composites were post-dried at 70°C.

Table II, respectively. The composites exhibited permanent deformation after removal of stress. As seen in Fig. 6, plastic deformation tended to occur to higher extent in the samples prepared from solutions of higher AC/TMOS ratios. Here again the fracture strain was larger than 8.0% for the composite samples from solution AC2 (Table II) where the strain was over the measurement limitation of the tester. The fracture strain increased from 3.9 ± 0.3 to over 8.0% as the AC/TMOS ratio increased from 0.5 to 2.0 (Table II). Young's moduli and bending strengths obtained from the curves are shown in Fig. 7 as a function of AC/TMOS ratio in the starting solutions. Young's modulus decreased by about 28% from 3.9 ± 0.2 to 2.8 ± 0.3 GPa when the AC/TMOS ratio increased from 0.5 to 2.0. The bending strength decreased by ca. 20%, from 100 ± 9 to 80 ± 6 MPa, with increasing AC/TMOS ratio from 0.5 to 2.0.

3.4. SEM observation and element analysis

Fig. 8 shows the SEM pictures of the fracture surface of the composites prepared from solutions of different

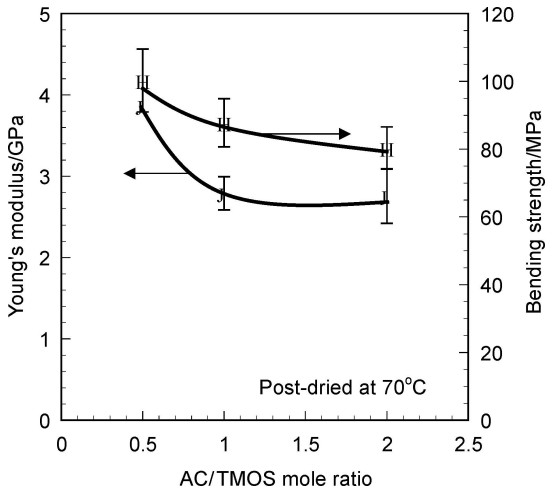

Figure 7 Young's modulus and bending strength of the composites plotted against AC/TMOS mole ratio. The composites were post-dried at 70°C.

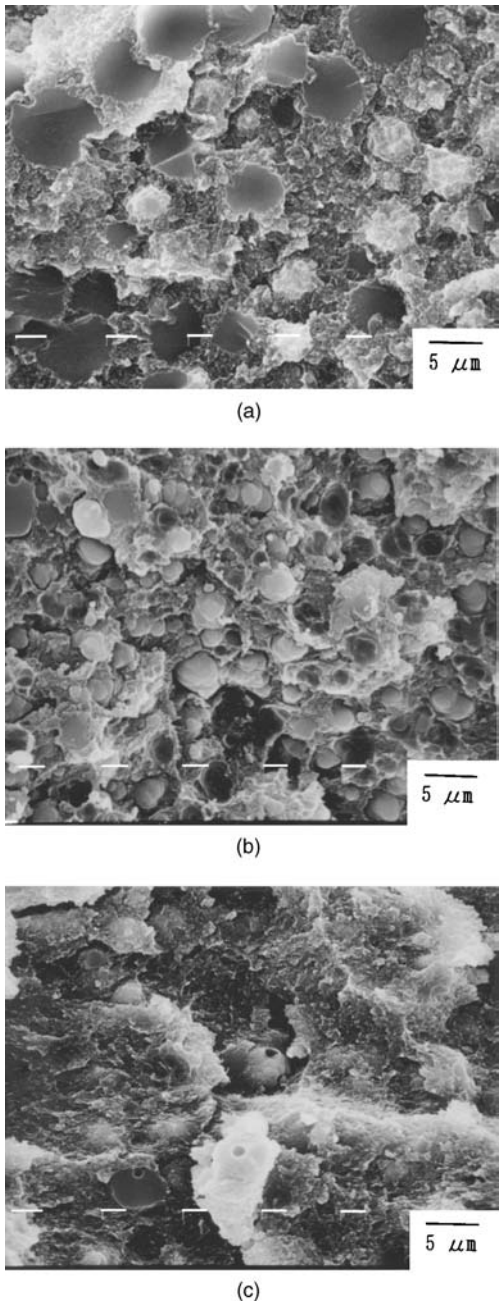

Figure 8 SEM photographs of the fracture surface of the composites post-dried at 70°C. AC/TMOS = (a) 0.5, (b) 1.0 and (c) 2.0.

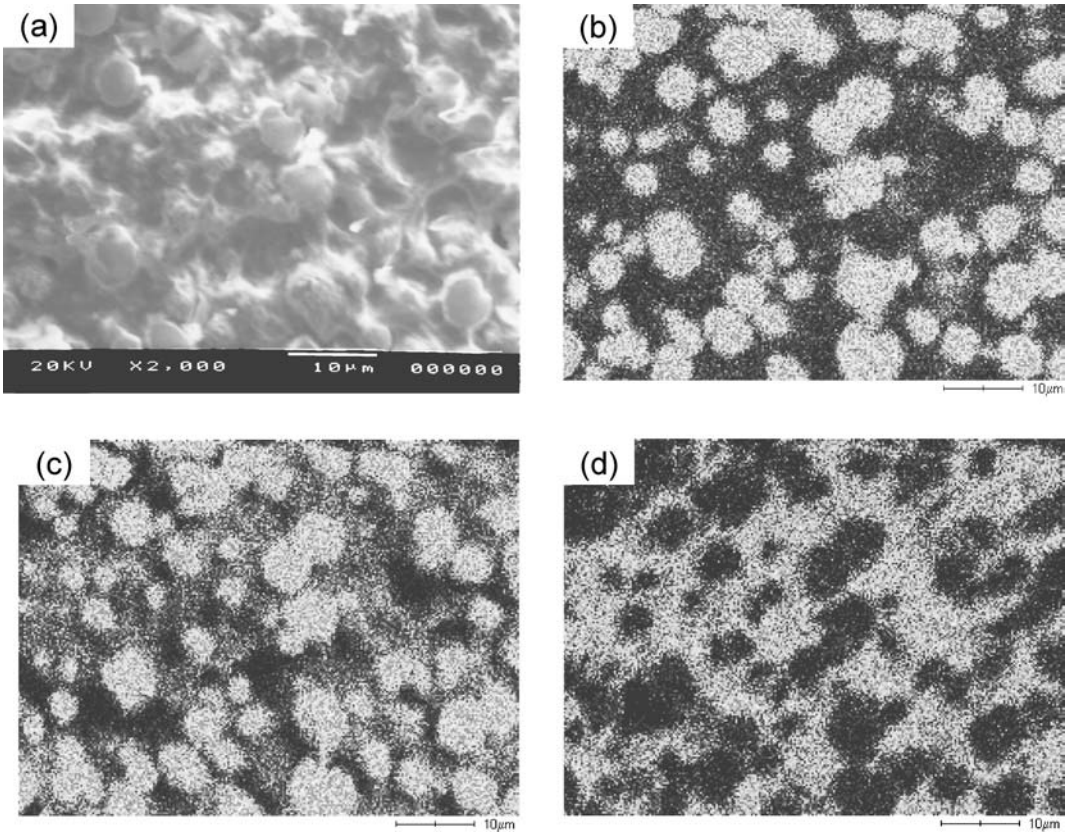

Figure 9 SEM image and corresponding two-dimensional elemental maps of the fracture surface of the sample prepared from solution AC0.5 and dried at 70°C. (a) SEM image, and elemental maps of (b) Si, (c) O and (d) C. Light spots represent those rich in the corresponding elements.

AC/TMOS ratios and post-dried at 70°C. The composites prepared from solutions of AC/TMOS = 0.5 and 1.0 had micrometer-sized particles dispersed in the matrices. The composites from solutions of AC/TMOS = 2.0, on the other hand, the interface between the particles and the matrix was indistinct or almost vanishing.

Figs 9 and 10 show the two-dimensional elemental maps obtained by EDX for the fracture surface of the composites prepared from solutions of AC/TMOS = 0.5 and 2.0, respectively. As is seen in Fig. 9, the specimen of AC/TMOS = 0.5 has the micrometer-sized particles rich in Si and O and poor in C, and the matrix poor in Si and O and rich in C. In other words, the specimen is composed of the micrometer-sized particles rich in silica and the matrix rich in AC. Phases rich in silica are also distributed in the matrix rich in AC in the specimen of AC/TMOS = 2.0 (Fig. 10). However, the interface between the particles and the matrix is less distinct than those in the specimen of AC/TMOS = 0.5.

4. Discussion

4.1. Formation of dried gels

The gel plates underwent warping on drying in the polypropylene containers when prepared from solutions without $CH_3OC_2H_4OH$, while they did not from solutions containing $CH_3OC_2H_4OH$. The volatile components in wet gels are THF, CH_3OH, which is the byproduct of TMOS hydrolysis, H_2O and $CH_3OC_2H_4OH$. The boiling points of THF, CH_3OH, H_2O and $CH_3OC_2H_4OH$ are 66, 64.7, 100 and 124.5°C, respectively. Therefore, the rate of vaporization would become relatively higher when the solution does not contain $CH_3OC_2H_4OH$. Rapid vaporization makes it difficult for structural relaxation to catch up with the increase in capillary pressure, which could lead to warping of the gel plate.

Without $CH_3OC_2H_4OH$, liquid phase rich in H_2O would be left behind in the gel pores in the course of vaporization of THF and CH_3OH. On the other hand, when the solution contains $CH_3OC_2H_4OH$, the liquid in pores becomes rich in $CH_3OC_2H_4OH$ during drying. H_2O has much higher surface tension (71.82 mN m^{-1}) than $CH_3OC_2H_4OH$ (33.30 mN m^{-1}), and the capillary pressure is proportional to the surface tension of the liquid [37]. Therefore, the capillary pressure could be much higher when the solution does not contain $CH_3OC_2H_4OH$, which could also induce gel plate warping.

In addition to what is mentioned above, when the solution does not contain $CH_3OC_2H_4OH$, vaporization occurs rapidly, which could allow the upper surface of the sol to be gelled prior to the gelation of the inner. This could provide distribution in the rate of vaporization and shrinkage, leading to warping of the gel plate.

Incorporation of $CH_3OC_2H_4OH$ was thus effective in obtaining warping-free dried gel plates because of the high boiling point particularly than water.

4.2. Microstructure of the composites

The EDX alaysis revealed that the composites are composed of silica-rich phases dispersed in AC-rich matrix (Figs 9 and 10). AC of 53–56% in acetylation was

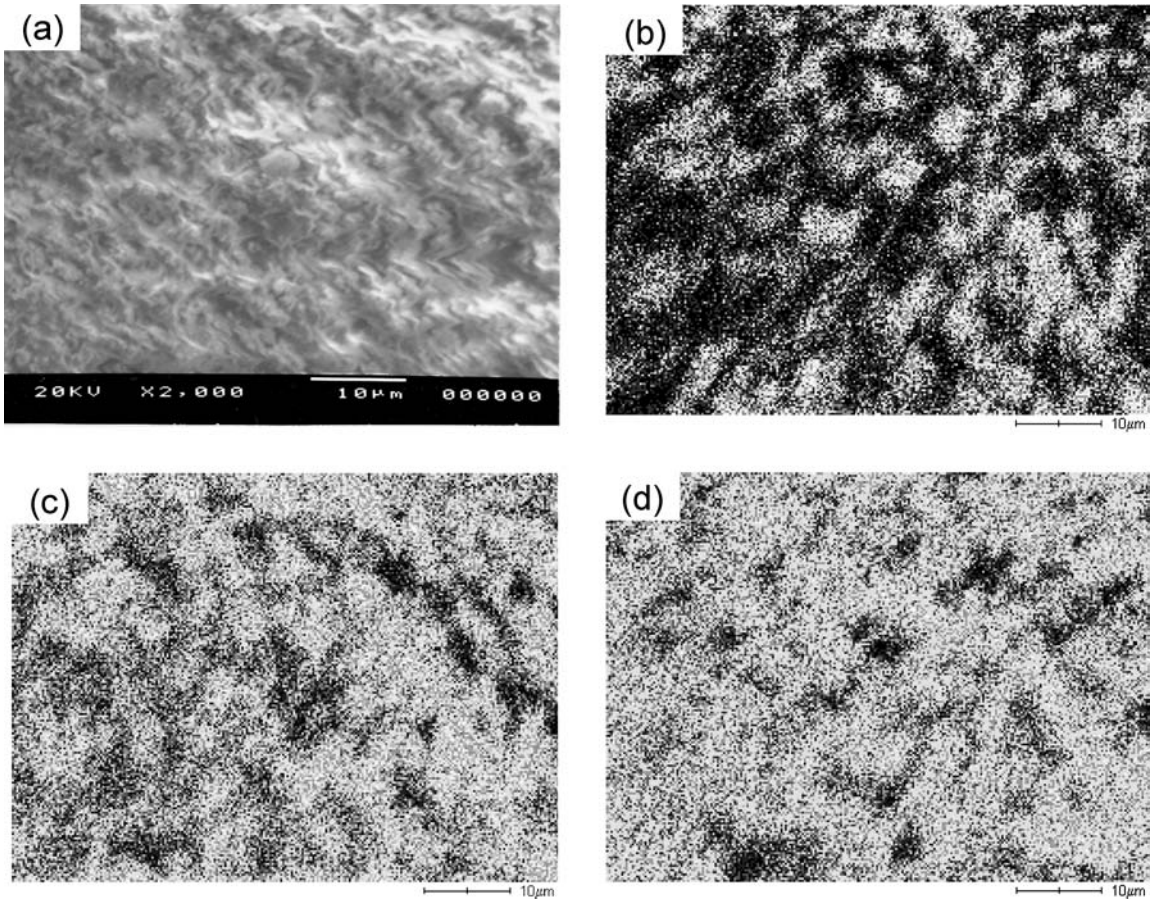

Figure 10 SEM image and corresponding two-dimensional elemental maps of the fracture surface of the sample prepared from solution AC2 and dried at 70°C. (a) SEM image, and elemental maps of (b) Si, (c) O and (d) C. Light spots represent those rich in the corresponding elements.

used in the present study, that is, about three of six OH groups are replaced by CH_3COO groups per cellulose monomer. Because the acetyl groups are hydrophobic rather than hydrophilic, AC cannot have strong interaction with the OH groups of the siloxane polymers. This could lead to the phase separation observed between silica-rich and AC-rich phases. The interface between the silica-rich and AC-rich phases was more distinct in the specimen of AC/TMOS = 0.5 than in that of AC/TMOS = 2.0 (Figs 9 and 10); the compositions of the former and the latter would be close to and far from the center of the miscibility gap in silica-AC system.

All the dried gels obtained were opaque while all the sols were transparent. The opacity appeared during drying. Light scattering both at the interface between the silica- and AC-rich phases and at the pores could be the origin of the opacity. The true density of SiO_2 glass and AC are 2.2 and 1.36 g cm^{-3}, respectively, and the bulk density of the composites obtained ranged from 1.22 to 1.37 g cm^{-3} (Figs 2 and 5). Therefore, the composites are concluded to be porous in nature.

4.3. Effects of the post-drying temperature and the AC/TMOS mole ratio on the mechanical properties of the composites

The extent of the plastic deformation decreased (Fig. 3), and Young's modulus and bending strength increased when the gels were post-dried at higher temperatures (Fig. 4). The bulk density of the composite samples, on the other hand, increased with increasing post-drying temperature (Fig. 2). This indicates that the increase in Young's modulus and strength, and the decrease in the degree of plastic deformation result from densification, which is promoted by post-drying at higher temperatures.

The plastic deformation tended to occur to larger extents as the AC/TMOS ratio in solution increased, where the plastic deformation proceeded over the yield point at AC/TMOS = 2.0 (Fig. 6). Also Young's modulus and bending strength decreased with increasing AC/TMOS ratio (Fig. 7). AC polymers have much higher flexibility than three-dimensional siloxane polymers. Therefore, the increase in the volume fraction of AC-rich matrix in the composites and/or the increase in the AC fraction in the matrix could provide the composites flexibility and could reduce the modulus and strength. The decrease in bulk density is also thought to contribute to the decreased modulus and strength. However, although the bulk density was similar between the composites prepared from solutions of AC/TMOS = 1.0 and 2.0 (Fig. 5), the composite sample from the solution of AC/TMOS = 2.0 showed plastic deformation to much larger extent (Fig. 6). As seen in the SEM pictures, the interface between the silica-rich particles and the AC-rich matrix was not clear at AC/TMOS = 2.0. Difference in the phase constitution and in the degree of hybridization between AC and siloxane polymers may affect the mechanical characteristics.

TABLE III Mechanical properties and shape of organic polymer/silica composites and the maximum temperature for drying. The mechanical properties of cortical bones are also shown

Component					Maximum temperature	
Organic	Inorganic	Young's modulus (GPa)	Strength (MPa)	Shape	for drying	References
AC	SiO_2	1.8–3.9	48–100[b]	Bulk (4.4 × 5 × 2 mm^3)	70°C	Present work
PMMA	SiO_2	1.0–1.2	64–87[b]	Bulk	40°C	[10]
HPC	SiO_2	0.2–0.6	6–18[t]	Film	60°C	[24]
PVAc	SiO_2	0.1–0.4	8–32[t]	Film	60°C	[25]
PI	SiO_2	2.7–3.5	45–143[t]	Film (ca.50 μm thick)	270°C	[27]
PDMS	SiO_2	0.06×10^{-3}–0.90×10^{-3}	0.06–0.79[t]	Film	–	[29]
PVA	SiO_2	2–3	80–115 [t]	Film	60	[30]
PTMO	SiO_2	5.2×10^{-3}–105×10^{-3}	1.1–31.3[t]	Film (10 mm long)	Room temp.	[31]
Cortical bone		7–30	50–150[b]			[3]

[b]bending strength.
[t]tensile strength.

The present composites had Young's moduli of 1.8–3.9 GPa and bending strengths of 48–100 MPa, depending on the drying temperature and AC/TMOS ratio in the starting solutions. These values are almost comparable to those of cortical bones (7–30 GPa in modulus and 50–150 GPa in bending strength) although the modulus is still slightly lower (Table III).

4.4. Comparison with other organic polymer/silica composites

Table III summarizes the mechanical properties of organic polymer/silica composites reported so far [10, 24, 25, 27, 29–31]. The maximum temperature for drying and the shape of the composites are also shown. As seen in the table, most of the composites experienced the maximum temperatures for drying similar to those employed in the present study, except for PI/silica composites. It is also noticed that the composites except for PMMA/silica were fabricated in the form of films. Because solvents can be vaporized more easily, higher densities and hence higher elastic constants or strengths would be achieved more readily in films. However, the data shown in the table indicate that the present monolithic AC/silica composites have Young's moduli and strengths comparable to or higher than the composite films, which is a valuable point achieved in the present study.

5. Conclusions

AC/silica composites were prepared from $Si(OCH_3)_4$ - AC - H_2O - HNO_3 - THF - $CH_3OC_2H_4OH$ in an attempt to realize mechanical properties similar to those of cortical bones.

(1) Crack-free, warping-free dried gel plates ca. 12 cm × 8 cm × 1 cm in size could be prepared. Incorporation of $CH_3OC_2H_4OH$ was inevitable in avoiding the warping occurring on drying.

(2) The composites, the dried gels, could be cut and polished without cracking or fracture, showing good machinability.

(3) The composites prepared from solutions of AC/TMOS = 0.5 and 1.0 were composed of micrometer-sized particles rich in silica surrounded by the matrix rich in AC. The composites from solutions of AC/TMOS = 2.0, on the other hand, the interface between the particles and the matrix was much less distincnt.

(4) Young's modulus and bending strength of the composites ranged in 1.8–3.9 GPa and 48–100 MPa, respectively, depending on the post-drying temperature and AC/TMOS mole ratio in the starting solutions.

(5) When the gels were post-dried at higher temperatures, the composites increased in bulk density, in Young's modulus and in bending strength accompanied by reduced degrees of plastic deformation.

(6) As the AC/TMOS ratio in solutions increased, the composites decreased in Young's modulus and in bending strength, with a decrease in the extent of plastic deformation.

Acknowledgments

This work is financially supported by Japan Society for the Promotion of Science (Grant-in-Aid for Exploratory Research).

References

1. B. BESIM and P. GIUSEPPE, *J. Ceram. Soc. Jpn.* **110** (2002) 601.
2. L. L. HENCH, *J. Am. Ceram. Soc.* **81** (1998) 1705.
3. T. KOKUBO, *Bull. Ceram. Soc. Jpn.* **30** (1995) 224 [in Japanese].
4. M. KOBAYASHI, T. NAKAMURA, Y. OKADA, W. F. MOUSA, S. SHINZATO, T. KOKUBO and T. KIKUTANI, in "Bioceramics," edited by H. Ohgushi, G. W. Hastings and T. Yoshikawa (World Scientific Publishing Co. Pte. Ltd., Singapore, 1999) Vol. 12, p. 417.
5. T. KASUGA, Y. OTA, S. OZAKI, M. NOGAMI and Y. ABE, in "Bioceramics," edited by H. Ohgushi, G. W. Hastings and T. Yoshikawa (World Scientific Publishing Co. Pte. Ltd., Singapore, 1999) Vol. 12, p. 437.
6. M. KAMITAKAHARA, M. KAWASHITA, N. MIYATA, T. KOKUBO and T. NAKAMURA, *J. Mater. Sci. Mater. Med.* **13** (2002) 1050.
7. N. MIYATA, Q. CHEN, T. KOKUBO and T. NAKAMURA, in "Bioceramics," edited by H. Ohgushi, G. W. Hastings and T. Yoshikawa (World Scientific Publishing Co. Pte. Ltd., Singapore, 1999) Vol. 12, p. 441.
8. Q. CHEN, N. MIYATA, T. KOKUBO and T. NAKAMURA, *J. Biomed. Mater. Res.* **51** (2000) 605.
9. Q. CHEN, F. MIAJI, T. KOKUBO and T. NAKAMURA, *Biomater.* **20** (1999) 1127.

10. K. TSURU, S. HAYAKAWA, C. OHTSUKI and A. OSAKA, Extended Abstract of the 2nd Symposium on Ceramics in Medicine, Biology and Biomimetics (The Ceramics Society of Japan, Kyoto, Japan, 1998) p. 16 [in Japanese].
11. S.-H. RHEE and J.-Y. CHOI, *J. Am. Ceram. Soc.* **85** (2002) 1318.
12. M. AIZAWA, Y. TSUCHIYA, K. ITATANI, H. SUEMASU, A. NOZUE and I. OKADA, in "Bioceramics," edited by H. Ohgushi, G. W. Hastings and T. Yoshikawa (World Scientific Publishing Co. Pte. Ltd., Singapore, 1999) Vol. 12, p. 453.
13. J. HUANG, L. D. SILVIO, M. WANG, I. REHMAN and C. OHTSUKI, *J. Mater. Sci. Mater. Med.* **8** (1997) 809.
14. W. BONFIELD, in "Bioceramics," edited by T. Kokubo, T. Nakamura and F. Miyaji (Elsevier Science, Oxford, 1996) Vol. 9, p. 11.
15. M. WANG, T. KOKUBO and W. BONFIELD, in "Bioceramics," edited by T. Kokubo, T. Nakamura and F. Miyaji (Elsevier Science, Oxford, 1996) Vol. 9, p. 387.
16. L. L. HENCH, *J. Am. Ceram. Soc.* **74** (1991) 1487.
17. Y. SHIKINAMI, K. HATA and M. OKUNO, in "Bioceramics," edited by T. Kokubo, T. Nakamura and F. Miyaji (Elsevier Science, Oxford, 1996) Vol. 9, p. 391.
18. M. KIKUCHI, Y. SUETSUGU, J. TANAKA and M. AKAO, in "Bioceramics," edited by T. Kokubo, T. Nakamura and F. Miyaji (Elsevier Science, Oxford, 1996) Vol. 9, p. 395.
19. H. MAEDA, T. KASUGA, M. NOGAMI, Y. HIBINO, K. HATA, M. UEDA and Y. OTA, *J. Mater. Res.* **17** (2002) 727.
20. K. TSURU, S. HAYAKAWA, C. OHTSUKI and A. OSAKA, *J. Mater. Sci. Mater. Med.* **9** (1998) 479.
21. Y. HU and J. D. MACKENZIE, *J. Mater. Sci.* **27** (1992) 4415.
22. J. D. MACKENZIE, *J. Sol-Gel Sci. Tech.* **2** (1994) 81.
23. J. D. MACKENZIE, Q. HUANG and T. IWAMOTO, *ibid.* **7** (1996) 151.
24. S. YANO, *Polymer* **35** (1994) 5565.
25. S. YANO, K. NAKAMURA, M. KODOMARI and N. YAMAUCHI, *J. Appl. Polym. Sci*. **54** (1994) 163.
26. Z. AHMAD and J. E. MARK, *Chem. Mater.* **13** (2001) 3320.
27. X.-Y. SHANG, Z.-K. ZHU, J. YIN and X.-D. MA, *ibid.* **14** (2002) 71.
28. J. E. MARK and S.-J. PAN, *Makromol. Chem. Rapid Commun.* **3** (1982) 681.
29. Y. P. NING, M. X. ZHAO and J. E. MARK, in "Chemical Processing of Advanced Materials," edited by L. L. Hench and J. K. West (John Wiley, New York, 1992) p. 745.
30. S. YANO, K. HURUKAWA, M. KOHAKU and K. KURITA, *Jpn. J. Polym. Sci. Techn.* **53** (1996) 218 [in Japanese].
31. H.-H. HUANG, R. H. GLASER and G. L. WILKES, in "Inorganic and Organometallic Polymers" (ACS Symposium Series 360) edited by M. Zelden, K. J. Wynne and H. R. Allcock (American Chemical Society, Washington D.C., 1988) p. 354.
32. S. KATAYAMA, Y. KUBO and N. YAMADA, *J. Am. Ceram. Soc.* **85** (2002) 1157.
33. C. OHTSUKI, T. MIYAZAKI, H. IWASAKI, S. OGATA and M. TANIHARA, in "Extended Abstract of the 13th Symposium on Reactivity of Solids," Suita, Japan, Nov. 14–15, 2002, p. 110. [in Japanese]
34. T. MIYAMOTO, S. TAKAHASHI, H. ITO, H. INAGAKI and Y. NOISHIKI, *J. Biomed. Mater. Res.* **23** (1989) 125.
35. A. OYANE, M. MINODA, T. MIYAMOTO, K. NAKANISHI, M. KAWASHITA, T. KOKUBO and T. NAKAMURA, in Proceedings of International Symposia on Materials Science for the 21st Century (ISMS-21) edited by N. Miyata, R. Ota, Y. Miyamoto and T. Shiono (Suita, Japan, 2001) Vol. B, p. 75.
36. T. TAKAHASHI and Y. NAKAYAMA, "Wood Science Series 3: Physics," 2nd ed. (Kaiseisha, Otsu, Japan, 1995) p. 147 [in Japanese].
37. C. J. BRINKER and G. W. SCHERER, "Sol-Gel Science" (Academic Press, San Diego, 1990) Chap. 7.

Received 27 February
and accepted 17 December 2004